Eur. Phys. J. A **9**, 293–297 (2000)

THE EUROPEAN PHYSICAL JOURNAL A

Short note

DSA lifetime measurements and structure of positive-parity bands of ^{120}Xe

A.A. Pasternak[1,a], Y. Sasaki[2], A.D. Efimov[1], V.M. Mikhajlov[3], T. Hayakawa[4], Y. Toh[4], M. Oshima[4], Y. Hatsukawa[4], J. Katakura[4], N. Shinohara[4], Z. Liu[5], and K. Furuno[2]

[1] Cyclotron Laboratory, A.F. Ioffe Physical Technical Institute, 194021, St. Petersburg, Russia
[2] Tandem Accelerator Center, University of Tsukuba, Tennoudai, Tsukuba 305-8577, Japan
[3] Physical Institute of St. Petersburg State University, 198904, St. Petersburg, Russia
[4] Japan Atomic Energy Research Institute, Tokai-mura, Naka-gun, Ibaraki 319-1195, Japan
[5] RIKEN, Wako-shi, Saitama 351-0106, Japan

Received: 29 June 2000 / Revised version: 14 October 2000
Communicated by D. Schwalm

Abstract. Lifetimes of excited states in ^{120}Xe have been measured by the Doppler-shift attenuation method in the ^{111}Cd(^{12}C,3n) reaction at a beam energy of $E = 56$ MeV. Lifetime values for 22 states were obtained. The excitation energies and $E2$-transition probabilities of the yrast band, γ-band and its continuation are interpreted in the framework of a version of IBFM (IBM + 2 q.p.). A reasonable description of the $B(E2)$ behavior in the backbending region is achieved.

PACS. 21.10.Tg Lifetimes – 21.60.Fw Models based on group theory – 23.20.Lv Gamma transitions and level energies – 27.60.+j $90 \leq A \leq 149$

1 Introduction

Transitional nuclei around mass number $A \approx 120$ are characterized by γ-softness and a strong interaction between collective and two-quasiparticle degrees of freedom in the backbending region $I^\pi \approx 10^+$–14^+. For the interpretation of band structures in the backbending and high-spin regions lifetime measurements are very important. In ^{120}Xe, however, only the lifetimes for the 2^+ to 8^+ yrast levels were known from Recoil distance Doppler-shift method (RDM) experiments [1–3], that are partly not consistent.

A detailed level scheme of ^{120}Xe up to $I^\pi = 28^+$ was established in ref. [4] using the ^{106}Pd(^{18}O,4n) reaction at $E = 75$ MeV, opening the possibility of lifetime measurements in medium and high-spin regions. We have obtained new data on the lifetimes in ^{120}Xe with the DSA method using a (^{12}C,3n) reaction, which is optimal to minimize the influence of the sidefeeding delay time. These data provide a good testing ground for theoretical models. The energies of excited states in ^{120}Xe and electromagnetic transition probabilities are compared with calculations within a new version of the interacting boson model which takes into account two-quasiparticle states [5]. In this paper we present and discuss results only for the positive-parity bands. Additional experimental materials and illustrations including data for some negative-parity bands as well as detailed description of the theoretical approach will be given in a forthcoming paper.

2 Experimental methods and results

In our experiment excited states of ^{120}Xe have been populated by the ^{111}Cd(^{12}C,3n) reaction at a beam energy of $E = 56$ MeV. A metallic thick foil of ^{111}Cd (30 mg/cm^2 and 94% enrichment) was used as a target. Emitted γ-rays were registered with the GEMINI ball [6] consisting of 12 Compton-suppressed Ge detectors positioned at 32° (2 detectors), 58° (2), 90° (4), 122° (2) and 148° (2) with respect to the beam direction. A total of 290 million events two- or higher fold were stored in magnetic tapes. The coincidence spectra gated on transitions below the transition of interest and the sums of these gated spectra in different combinations were analyzed. For the cases of 16^+ yrast level spectra gated on transitions above it were used. The Doppler-broadened γ-lines measured at 58°, 90° and 122° were used for the DSA analysis.

The analysis of the experimental lineshapes was carried out using an updated version of the package of computer codes COMPA, GAMMA and SHAPE [7,8]. With the help of this software it is possible to handle, in partic-

[a] e-mail: alexandr@alpas.ioffe.rssi.ru

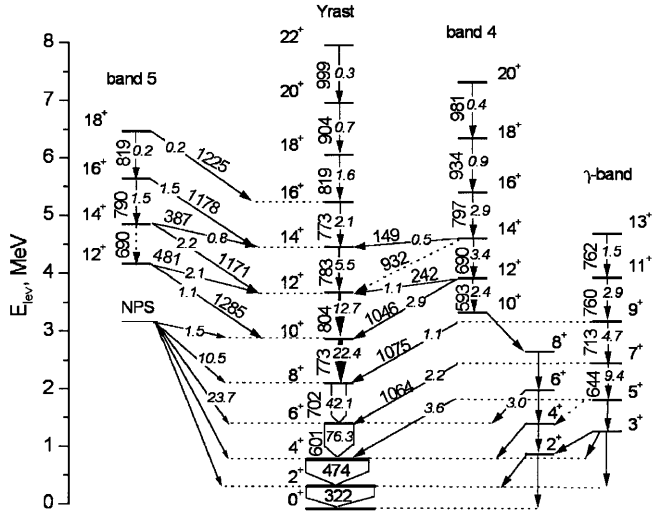

Fig. 1. Partial level scheme of ^{120}Xe [4]. Relative intensities measured in this work and normalized to the 322 keV line are given in italics. NPS represent all negative-parity states, which feed the yrast band. The sums of intensities from these levels are presented.

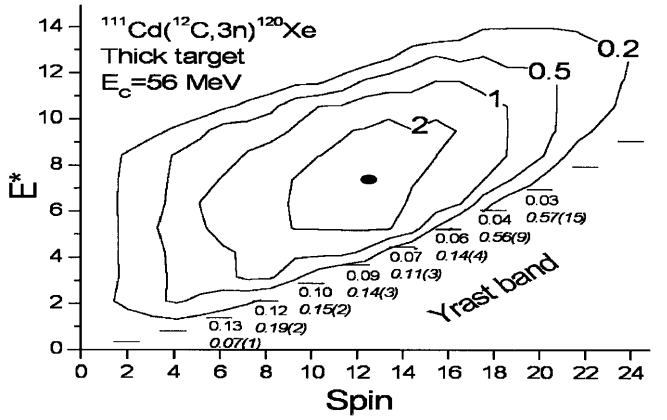

Fig. 2. Entry state population distribution as derived by Monte Carlo calculation. The value of $\tau_{\rm sf}$ is given under each yrast level. Below, in italics, the side-feeding intensities, normalized to the total outgoing intensity, are presented.

ular, groups of interfering Doppler-broadened peaks using lifetimes as lineshape parameters. For the stopping power of the recoils Lindhard correction factors for electronic ($f_{\rm e}$) and nuclear ($f_{\rm n}$) components were assumed as $f_{\rm e} = 1.27 \pm 0.07$ and $f_{\rm n} = 0.77 \pm 0.07$ taken from [7,8] for the ^{119}I – ^{109}Ag recoil-target combination, where these parameters were determined by Doppler-shift lineshape analysis using the "semi-thick target" method. Cascade feeding have been taken into account using the level scheme from ref. [4]. (A partial scheme, important for the lifetime evaluation, is presented in fig. 1.) Intensities of transitions have been carefully measured by taking into account Doppler broadening effect. Some details of the lifetime evaluation procedure are described in refs. [8,9].

In fig. 2 the entry state population distribution is presented. The calculation was performed with Monte Carlo methods using the program COMPA. Since we used a thick target, the two-dimensional (energy-spin) position of the maximum of population, marked as a black dot in the picture, is located near (7.5 MeV-12$\hbar$). Under these conditions the delay time due to sidefeeding at high spins is determined mainly by fast statistical dipole transitions and is expected to be very short. As the spins of the investigated states decrease, $\tau_{\rm sf}$ should become larger due to an increased length of the sidefeeding and to an admixture of stretched $E2$ cascades. For comparison in the case of ^{119}I where a similar reaction, ^{109}Ag(^{13}C,3n)^{119}I at $E_{\rm C} = 54$ MeV was used [8,9], the energy-spin position of the maximum of population distribution was (13 MeV-18$\hbar$) and for the high-spin region of $I \approx 16$–18, $\tau_{\rm sf}$ has been experimentally evaluated by precise lineshape analysis to be $\tau_{\rm sf} \approx 0.10$ ps. In the present case, the 818.7 keV line corresponding to the $18^+ \longrightarrow 16^+$ yrast band transition was used for two-dimensional $(\tau, \tau_{\rm sf})$ fitting. As a result, a sidefeeding delay of $\tau_{\rm sf} = 0.040 \pm 0.015$ ps has been found. In ref. [9] a simple empirical method for the extrapolation of $\tau_{\rm sf}$ to another yrast level is proposed. The results of the calculations together with relative sidefeeding intensities are presented in fig. 2. Since the measured and extrapolated $\tau_{\rm sf}$ values are much smaller than the lifetimes of the investigated levels, our results for the lifetime measurements are practically independent of the details of the sidefeeding pattern.

A complex case in the lifetime evaluation is the doublet of 773.7 keV, corresponding to the $10^+ \longrightarrow 8^+$ and $16^+ \longrightarrow 14^+$ transitions in the yrast band (fig. 3). As first step we have evaluated τ of the 16^+ level from the upper gate 819 keV, where the intensities of both transitions have to be equal. To reduce the influence of the stopped components of 819 keV and upper transitions, the gate was only set on the Doppler-shifted parts of the 819 keV line at the 58° and 122° angles in the energy range of 822–826 keV and 812–816 keV, respectively. (Gate 819 flight in table 1.) The effective lifetime of the 10^+ state due to the long cascade feeding was estimated as $\approx 5 \pm 2$ ps and corresponding lineshapes should be close to the apparatus lineshape of the Ge detector. The energy positions of both components have been checked using the 90° spectrum and turn out to be equal ($\Delta E \leq 0.15$ keV). Under these conditions the relative intensities and energy positions of both peaks have been fixed as equal during the fitting procedure and only one parameter, $\tau(16^+)$, had to be evaluated (table 1). The lifetime of the 10^+ state can be evaluated from bottom gates using the facts that the intensity of the $16^+ \longrightarrow 14^+$ transition should be significantly less compared to that of the $10^+ \longrightarrow 8^+$ one and that $\tau(16^+)$ is known. For the determination of the relative intensities the spectra gated on the 804 keV ($12^+ \longrightarrow 10^+$) line have been used. In this gate the intensities of the $10^+ \longrightarrow 8^+$ (773 keV) and $8^+ \longrightarrow 6^+$ (702 keV) transitions have to be equal, but due to a contribution of the $16^+ \longrightarrow 14^+$ line the intensity of the 773.7 keV doublet has to exceed the intensity of the 702 keV line.

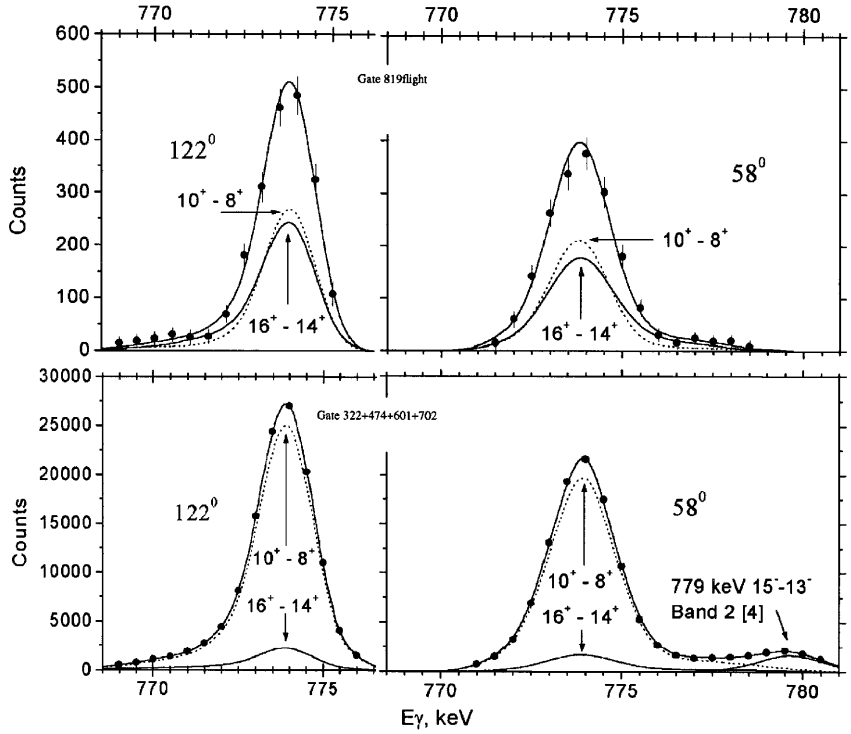

Fig. 3. Lineshape analysis of the 773.7 keV $10^+ \longrightarrow 8^+$ and $16^+ \longrightarrow 14^+$ doublet of the yrast band. See text.

Therefore the intensity of the $16^+ \longrightarrow 14^+$ line can be found and normalized to the 819 keV ($18^+ \longrightarrow 16^+$) transition. Since this ratio should be the same for all bottom yrast band gates, we finally found the intensity ratio $I(16^+ \longrightarrow 14^+)/I(10^+ \longrightarrow 8^+) = 0.095 \pm 0.015$ and subsequently $\tau(10^+)$ has been evaluated from the sum of the gates on the 322, 474, 601 and 702 keV lines (fig. 3).

Results of the lifetime measurements for 22 positive-parity levels are presented in table 1. One can compare our data for the 6^+ and 8^+ states with previous results obtained with the RDM: 2.5 ± 0.3 ps for the 6^+ level [1] and, respectively, 0.9 ± 0.4 ps [2] and 1.2 ± 0.2 ps [3] for the 8^+ level.

3 Discussion

Spectra of many Xe, Ba, Ce nuclei possess some common features that indicate a collectivity of these nuclei and explicitly display the interaction between the collective quadrupole mode and the high-spin two-quasiparticle excitations involving $h_{11/2}$ quasiparticles. This interaction leads to a fragmentation of the collectivity over several high-spin states for energies of the order of the double-pairing gap. This is confirmed by theoretical considerations. A number of investigations ([4,10] and references therein) used approaches based on shape coexistence. In ref. [5] level structure of nuclei in this mass region was analyzed with a version of IBFM in which a possible shape instability was taken into account by means of variations of the collective operator parameters. As the energies and angular momenta increase, the structure of the collective quadrupole excitations can change. The excitation of high-spin two-quasiparticle pairs intensifies this change narrowing the collective space and bringing additional variations in the mean field and pairing. In the phenomenological framework of IBM we take these alterations into account by using different sets of IBM parameters in boson images of operators. The first set of the IBM1-Hamiltonian parameters is fitted for a relatively small spin region ($I \leq 8$), up to the bandcrossing, where two-quasiparticle configurations are practically absent. The second set is found for high-spin states in which two-quasiparticle components are explicitly present *i.e.* after the bandcrossing.

This phenomenological aspect of the approach has been developed in ref. [5]: detailed microscopic considerations of the interaction between collective quadrupole phonons, fermion counterparts of IBM d-bosons, and two-quasiparticle phonons are used instead of simple two-quasiparticle states introduced in the original version of IBFM for even nuclei [11]. The phonon structure and energies are calculated in the framework of RPA with standard single-particle energies, pairing gaps corresponding to even-odd mass differences and with factorized multipole forces. The phonons with spins $L = 4$, 6 involve several two-quasiparticle components, whereas phonons with $L = 8$, 10 are practically pure $(h_{11/2})^2$ configurations.

The comparison of the theoretical and experimental energy spectra is presented in fig. 4. The reproduction of the yrast levels up to $I = 18$ is satisfactory as the differences between theoretical and experimental energies are not greater than 50 keV except for the 12^+ yrast level (discrepancy ≈ 200 keV). For the yrast states with $^{++}I \leq 10$ the collective components prevail ($\geq 60\%$). On the con-

Table 1. Lifetimes of excited states of ^{120}Xe.

$J^\pi_{\rm Band}$	E_γ (keV)	τ (ps)	θ, gate	$J^\pi_{\rm Band}$	E_γ (keV)	τ (ps)	θ, gate
$6^+_{\rm yr}$	601	$2.05^{+0.65}_{-0.40}$	b g2	16^+_4	797	$0.65^{+0.27}_{-0.13}$	b g3a
$8^+_{\rm yr}$	702	1.32 ± 0.25	b g3	18^+_4	934	0.32 ± 0.07	b, f g3a
$10^+_{\rm yr}$	773	0.91 ± 0.15	b, f g4	20^+_4	981	0.17 ± 0.06	f g7
$12^+_{\rm yr}$	804	0.84 ± 0.13	b, f g4	12^+_5	481	$0.84^{+0.20}_{-0.15}$	f g1c
$14^+_{\rm yr}$	783	1.00 ± 0.15	b, f g1a	14^+_5	1171	0.31 ± 0.05	b, f g5
$16^+_{\rm yr}$	773	$0.69^{+0.22}_{-0.12}$	b, f g1b	16^+_5	790	$0.7^{+0.3}_{-0.1}$	b, f g4a
$18^+_{\rm yr}$	819	0.38 ± 0.06	b, f, p g3a	18^+_5	1225	$0.32^{+0.13}_{-0.07}$	b, p g3a
$20^+_{\rm yr}$	904	0.18 ± 0.04	b, f, p g3a	7^+_γ	1064	$0.9^{+0.5}_{-0.2}$	b g1
$22^+_{\rm yr}$	999	0.13 ± 0.06	b, f, p g3a	9^+_γ	1075	0.75 ± 0.10	b g1
12^+_4	1046	$1.8^{+1.4}_{-0.4}$	f g1d	11^+_γ	760	$0.8^{+0.3}_{-0.2}$	f, b g4
14^+_4	690	$1.6^{+0.7}_{-0.4}$	b, f g5	13^+_γ	762	$1.25^{+0.32}_{-0.24}$	f g3

b: $\theta = 122°$; f: $\theta = 58°$; p:$\theta = 90°$; g1: 322 keV; g2: (322+474) keV; g3: (322+474+601) keV; g4: (322+474+601+702); g5: (322+474+601 +702+773) keV; g1a: 804 keV; g1b: 819 flight; g1c: 474 keV; g1d: 773 keV; g3a: (773+804+782) keV; g4a: (601+702+773+804) keV; g7: (322+474+601+702+773+804+782) keV.

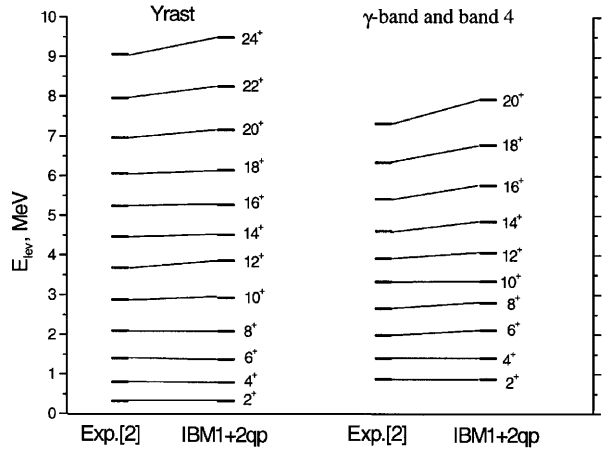

Fig. 4. Comparison of experimental and theoretical energy spectra.

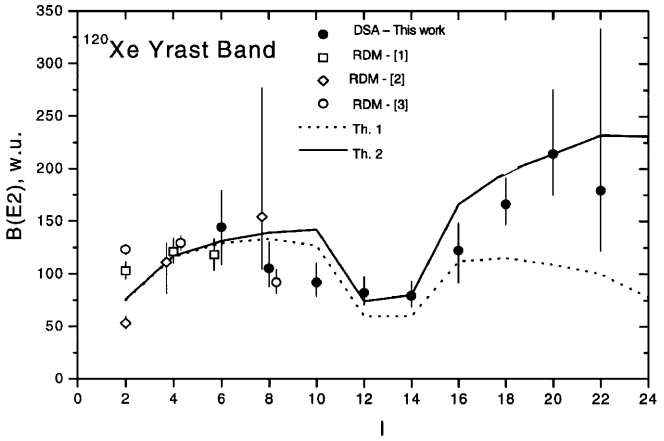

Fig. 5. Experimental and theoretical $B(E2)$ values for the yrast states.

trary, the states with $I \geq$14 are built on 10^+ $\nu(h_{11/2})^2$ excitations. The 12^+ state is transitional: s-, d- collective and two-quasiparticle components are uniformly mixed. The description of the γ-band and its continuation, shown in fig. 4, can be regarded as satisfactory at least up to $I = 12$. The γ-band states being at low spin ($\leq 6^+$) almost purely collective acquire essential two-quasiparticle components with spins 4^+, 6^+, 8^+ for band 4 states with $I \geq 8^+$ and are thereby transformed into the purely two-quasiparticle band 4.

The approach taking into account the dependence of the IBM parameters on the presence of two-quasiparticle phonons allows to determine the parameters of the $E2$ transition operators. To describe $E2$-probabilities in the framework of IBM1, we normalize the IBM1 $E2$-operator as to exactly reproduce the $B(E2)$ value of the 4^+ yrast level. We obtained reasonable $B(E2)$ values for yrast states up to 12^+ and, possibly, even up to 16^+. These calculations are presented in table 2 and fig. 5 as Th. 1.

The experimental $B(E2)$ values after the bandcrossing ($I \geq 16$) given in fig. 5 indicate that for higher spins the usual approach of IBM1 leads to an underestimation of the $B(E2)$ values. This is in agreement with the analysis of $B(E2)$ values in refs. [5,12], where it has been shown that the well-known form of the IBM1 $E2$ transition operator cannot describe all peculiarities of the $E2$ transition probabilities, thus demanding a modification of this operator. To explain the experimental observation, we considered either to include additional terms in the $E2$ transition operator, thus producing an increase of the $E2$ matrix elements or to suggest that the maximum boson number of IBM can depend on the energy and structure of the excited states. Here we applied as a limit case the possibility of almost removing the dependence of this operator on the s-boson:

$$\mathrm{d}^+\mathrm{s} + \mathrm{s}^+\mathrm{d} + \chi(\mathrm{d}^+\mathrm{d})^{(2)} \longrightarrow \mathrm{d}^+ + \mathrm{d} + \chi(\mathrm{d}^+\mathrm{d})^{(2)}.$$

Table 2. Experimental and calculated $B(E2)$ for ^{120}Xe.

$I_i^\pi \longrightarrow I_f^\pi$	$B(E2)$, W.u.			$I_i^\pi \longrightarrow I_f^\pi$	$B(E2)$, W.u.		
	Exp.	Th1	Th2		Exp.	Th1	Th2
$4^+_{yr} \longrightarrow 2^+_{yr}$	$116 \pm 5^*$	116	117	$20^+_{yr} \longrightarrow 18^+_{yr}$	214^{+61}_{-39}	109	214
$6^+_{yr} \longrightarrow 4^+_{yr}$	144 ± 35	129	131	$22^+_{yr} \longrightarrow 20^+_{yr}$	179^{+154}_{-57}	100	232
$8^+_{yr} \longrightarrow 6^+_{yr}$	105^{+25}_{-17}	133	139	$12^+_4 \longrightarrow 10^+_4$	71^{+20}_{-31}	56	79
$10^+_{yr} \longrightarrow 8^+_{yr}$	92^{+18}_{-13}	127	142	$12^+_4 \longrightarrow 10^+_{yr}$	$4.6^{+1.3}_{-2.0}$	0.5	0.4
$12^+_{yr} \longrightarrow 10^+_{yr}$	82^{+15}_{-11}	60	74	$14^+_4 \longrightarrow 12^+_4$	68 ± 22	102	157
$14^+_{yr} \longrightarrow 12^+_{yr}$	79^{+14}_{-10}	60	80	$14^+_4 \longrightarrow 12^+_{yr}$	< 4	2.4	3.3
$16^+_{yr} \longrightarrow 14^+_{yr}$	122^{+26}_{-30}	112	166	$16^+_4 \longrightarrow 14^+_4$	111^{+25}_{-33}	133	199
$18^+_{yr} \longrightarrow 16^+_{yr}$	166^{+25}_{-19}	115	197	$18^+_4 \longrightarrow 16^+_4$	102^{+29}_{-18}	107	218

$*$ RDM [1–3] has been adopted.

This approximation which has proven to be useful for high-spin states may indicate that the maximum boson number of IBM depends not only on the number of the valence nucleons, but also on the spin of the state. The full line in fig. 5 shows the results of our calculations (Th. 2) in which the $E2$ transition operator without s-bosons is used for the calculation of the $E2$-matrix elements between components including two-quasiparticle pairs. The use of this operator does practically not change the theoretical $B(E2)$ values of the transitions between band 4 and the yrast band, in particular both variants give rather small values for the $12_2 \longrightarrow 10_1$ and $14_2 \longrightarrow 12_1$ transitions in agreement with experiment.

In spite of a general satisfactory description of the experimental results, there are some indications that point towards limitations of the present version of the calculations:

The facts that the calculated energy position of the 12^+ yrast state noticeably (200 keV) exceeds the experimental value and the distances between the experimental and calculated levels grow with I for $I > 18$ indicate that an improvement of the results could be obtained only by extending our configuration space, in particular by taking into account of 4-qp components. For the same reason band 5 was not described in these calculations.

We have not obtained agreement between the experimental and theoretical $B(E2)$ values in detail, in particular for the $8^+ \longrightarrow 6^+$, $10^+ \longrightarrow 8^+$ transitions in the yrast band and for the transitions in band 4 states with $I \geq 14$ with an almost identical structure of the collective wave functions (table 2). This indicates the necessity of developing a more sophisticated form of the $E2$-operator.

The descriptions of odd-spin levels of the γ-band and some negative-parity bands as well as the calculation of $M1$ transition probabilities are in progress now. To overcome the limitations and difficulties peculiar to the present variant of the theory will possibly require to leave the framework of the IBM description for collective excitations.

4 Conclusions

The lifetimes of 22 positive-parity levels up to 22^+ state in ^{120}Xe were obtained by DSAM with the (^{12}C,3n) reaction. Calculations taking into account the interaction of IBM1 bosons with two-quasiparticle phonons satisfactory reproduce the energy levels of the positive-parity bands up to spin 18^+. The explanation for increasing the $E2$-probabilities after backbending in the yrast band indicates that the maximum boson number of IBM can depend on the energies and structures of the excited states.

We would like to thank Prof. A. Gelberg and Prof. R. Lieder for discussions and critical remarks.

References

1. J. C. Walpe et al., Phys. Rev. C **52**, 1792 (1995).
2. W. Kutschera et al., Phys. Rev. C **5**, 1658 (1972).
3. A. Dewald et al., Z. Phys. A **334**, 163 (1989).
4. S. Tormanen et al., Nucl. Phys. A **572**, 417 (1994).
5. A. D. Efimov and V.M. Mikhajlov, Phys. Rev. C **59**, 3153 (1999).
6. K. Furuno et al., Nucl. Instrum. Meth. A **421**, 211 (1999).
7. I. Kh. Lemberg, and A.A. Pasternak, *Modern Methods in Nuclear Spectroscopy*, (Nauka L., 1985).
8. Yu. N. Lobach et al., Acta Phys. Polonica B **30**, 1273 (1999).
9. J. Srebrny et al., Nucl. Phys. A (2000) in press.
10. P. Petkov et al., Nucl. Phys. A **640**, 293 (1998).
11. N. Yoshida, A. Arima and T. Otsuka, Phys. Lett. B **114** , 86 (1982).
12. D. Vretenar et al., Phys. Rev. C **57**, 675 (1998).